

# Heterogeneity in the Composition and Catabolism of Indigenous Microbiomes in Subsurface Soils Cocontaminated with BTEX and Chlorinated Aliphatic Hydrocarbons

Kaiwen Yang, Lei Zhang, Azariel Ruiz-Valencia, Xin Song, Timothy M. Vogel, and Xiaojun Zhang\*

Cite This: <https://doi.org/10.1021/acs.est.4c10071>

Read Online

ACCESS |

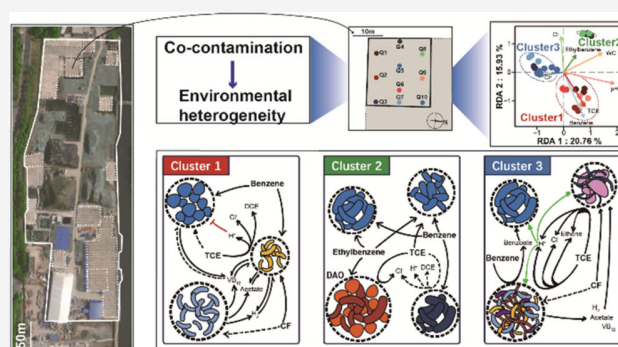
Metrics & More

Article Recommendations

Supporting Information

**ABSTRACT:** The effectiveness of in situ bioremediation can be affected by an insufficient understanding of high site/soil heterogeneity, especially in cocontaminated soils and sediments. In this study, samples from multiple locations within a relatively small area ( $20 \times 20 \text{ m}^2$ ) contaminated with benzene, toluene, ethylbenzene, and xylene (BTEX) and chlorinated aliphatic hydrocarbons (CAHs) were compared to examine their physicochemical and microbial properties. Unsupervised clustering analysis of 16S rRNA gene amplicon and metagenome shotgun sequencing data indicates that the indigenous community differentiated into three distinct patterns. In Cluster 1, *Pseudomonas*, with multiple monooxygenases and glutathione S-transferase (GST), was enriched in samples contaminated with high concentrations of BTEX and CAHs. Cluster 2 contained a high fraction of cometabolic degraders. Cluster 3 was dominated by *Ralstonia* and organohalide-respiring bacteria (OHRBs) mediating the reductive dechlorination of CAHs. Significant differences in composition and function among microbiomes were attributed to the differential distribution of organic pollutants, even in such a small area. Incorporating genomic features with physicochemical data can significantly enhance the understanding of the heterogeneities in soil and their impacts on microbial communities, thereby providing valuable information for the optimization of bioremediation strategies.

**KEYWORDS:** CAHs, BTEX, cocontamination, microbiomes, functional genes



## INTRODUCTION

Anthropogenic activities such as improper disposal, poor management, and long-term storage have led to the release of organic pollutants, including volatile organic compounds (VOCs).<sup>1</sup> Among these pollutants, aromatic compounds such as benzene, toluene, ethylbenzene, xylene (BTEX), and chlorinated aliphatic compounds (CAHs), including trichloroethene (TCE) and tetrachloroethene (PCE), are the most prevalent contaminants worldwide.<sup>2</sup> BTEX compounds have been classified as carcinogens (among these aromatic compounds, benzene has been identified as a type 1 carcinogen) and exert significant toxic effects, such as carcinogenicity, mutagenicity, and teratogenicity.<sup>3–5</sup> CAHs are also considered potential carcinogens and are listed as priority pollutants by the U.S. Environmental Protection Agency.<sup>6</sup> The co-occurrence of CAHs and BTEX in contaminated sites, particularly in industrial zones, has been widely documented.<sup>7–9</sup> This complicates the remediation process due to the divergent biodegradation pathways required for the different contaminants.

Several remediation strategies have been developed for contaminated sites,<sup>10,11</sup> among which microbe-mediated

bioremediation is widely regarded as a cost-effective and environmentally sustainable approach. The biodegradation of contaminants can occur via oxidative or reductive pathways depending on the chemical properties of contaminants and local environmental conditions. For example, highly chlorinated PCE and TCE are degraded via anaerobic reductive dechlorination, a process that requires reduced conditions, a sufficient supply of the cofactor cobalamin, an essential cofactor for the maturation and function of reductive dehalogenase, and the activity of organohalide-respiring bacteria (OHRBs). Depending on whether their growth relies exclusively on the energy released from the C–Cl bond via organohalide respiration, these bacteria are classified as either obligate or facultative OHRBs.<sup>12–1314</sup> Obligate OHRBs, such

Received: September 21, 2024

Revised: February 15, 2025

Accepted: February 18, 2025

as *Dehalococcoides* and *Dehalogenimonas*, can reduce chlorinated compounds completely to produce ethene, a nontoxic end product.<sup>14</sup> In contrast, facultative OHRBs only partially reduce chlorinated compounds, often yielding the toxic intermediate forms dichloroethylene and vinyl chloride. For CAHs with fewer chlorine substituents, the carbon scaffold and associated electrons are less protected and are thus more accessible to oxidative enzymes, such as alkene monooxygenase (AkMO) and epoxyalkane:coenzyme M transferase (Ea-CoMT).<sup>15–17</sup>

BTEX is biodegradable under both oxic and anoxic conditions. Research has shown that several aerobic bacterial lineages, including *Pseudomonas*, *Rhodococcus*, *Acinetobacter*, *Bacillus*, *Comamonas*, and *Microbacterium*, are able to utilize BTEX as the sole electron donor and carbon source.<sup>18,19</sup> Monooxygenases and dioxygenases play an important role in this process as they catalyze the hydroxylation reaction during which oxygen is introduced into the aromatic structure. In addition, iron-, nitrate-, and sulfate-reducing bacteria, including *Azoarcus*, *Thauera*, *Geobacter*, *Sulfurovum*, *Desulfovibrio*, *Cryptanaerobacter*, and *Pelotomaculum*, can anaerobically degrade BTEX in specific reductive anoxic environments. Their reductive functions are coupled with the anaerobic oxidation of BTEX, which can be catalyzed by anaerobic benzene carboxylation (*abcA* and *ancA*)<sup>20,21</sup> or fumarate addition (*assA* and *bssA*).

Previous studies have primarily addressed the bioremediation of individual contaminants and isolated degradation pathways and have neglected the complexities of cocontamination and the effects of effect of different types of contaminants on microbial community structure and function. Co-metabolic processes offer a promising solution for the bioremediation of cocontaminated sites.<sup>22</sup> Some BTEX degraders can oxidatively degrade CAHs, as enzymes that catalyze the oxidation of BTEX can also function when CAHs act as substrates.<sup>23</sup> Research on the mechanism of the cometabolic oxidation of CAHs and BTEX indicates that the populations responsible for this biological process consist of functional members that carry nonspecific monooxygenases.<sup>24–27</sup>

Given the diversity of biodegradation pathways under different scenarios, there is currently limited research on how microbial communities adapt to cocontamination and which pathway is favored. Efforts have been made to develop an efficient bioremediation approach utilizing combined chemical analysis and sequencing techniques to establish correlations and identify bioremediation targets.<sup>28</sup> Unfortunately, the distribution of pollutants and their potential combination effects are usually neglected in previous studies. Identifying the predominant pathway of pollutant removal and determining the underlying mechanisms is crucial for evaluating the feasibility of certain bioremediation strategies. In addition, the heterogeneous distribution of organic matter is the key factor in shaping community heterogeneity,<sup>29</sup> but little is understood regarding the effects of mixed organic contaminants on microbial communities and to what extent these microbial communities may diverge at the meter-scale within contaminated sites.

The current study evaluated the compositional and functional heterogeneity of native microbial communities present in subsurface soil samples collected from 10 sampling locations spanning an area of 400 m<sup>2</sup> situated within a cocontaminated industrial zone. The goals of this study were to demonstrate

the spatial heterogeneity of biodegradation pathways and present a hypothetical mechanism underlying the formation of different patterns.

## MATERIALS AND METHODS

**Soil Sampling.** Soil samples were collected from a 20 × 20 m<sup>2</sup> contaminated industrial site located in Suzhou, Jiangsu, China (31°16'N, 120°38'E, Figure S1). This site was a chemical plant, and previous site investigations have revealed the presence of CAHs and BTEX compounds in this area. The primary contaminants identified at the study site are CAHs, including carbon tetrachloride, trichloromethane, dichloromethane, 1,1,2-trichloroethane, PCE, TCE, 1,1-dichloroethylene, cis-1,2-dichloroethylene, and vinyl chloride, as well as benzene and ethylbenzene (Figure S2). A contamination hotspot was detected in the groundwater (15.0–18.5 m) in silty sand. The groundwater flowed from northeast to southwest.

Soil samples weighing 3–5 kg were collected from 10 locations at a depth of 10–12.5 m in this site using GeoProbe Systems (GeoProbe Inc.). Soil samples were placed in sterile plastic self-sealing bags, frozen, and transported on ice to the laboratory, where the samples were immediately stored at –80 °C. Each sample was subsampled once for chemical analyses and in triplicate for pH measurements and DNA extraction.

**DNA Extraction and Sequencing.** DNA samples for amplicon sequencing were extracted from 0.5 g of soil for each of the 30 soil samples (triplicates at each point) with Fast DNA SPIN Kit (MP Biomedicals) following the manufacturer's instructions. All 30 of the soil DNA samples were utilized for amplicon sequencing library preparation. In brief, the V3–V4 hypervariable regions of the 16S rRNA genes were amplified using conventional polymerase chain reaction (PCR) with the universal primers 341F (5'-CCTACGGGNGGCWGCAG-3') and 785R (5'-GACTACHVGGGTATCTAATCC-3').<sup>30</sup> Amplicon library preparation was conducted following the manufacturer's instructions (Part #15044223Rev.B; Illumina Inc.) with modifications as previously described.<sup>31</sup> After mixing the purified products obtained from the second-round amplification in equal quantities, the amplicon library was prepared with the MiSeq Reagent Kit v3. High-throughput sequencing was performed using the Illumina MiSeq platform (Illumina, Inc.). Due to the low biomass in the soil and the extraction of insufficient DNA for metagenomic library construction, the microbiome in the original soil samples was enriched by adding 10 mM sodium lactate and 1 mM TCE prior to metagenomic sequencing. Preincubation followed a previously described method<sup>32</sup> (Appendix S1). After 10 days of enrichment, DNA samples were extracted from the soil slurries. Library preparation and metagenomic sequencing were conducted by Personalbio (Shanghai) to generate paired-end 2 × 150 bp reads with NovaSeq (Illumina, Inc.).

**Sequencing Data Processing.** MiSeq paired-end sequencing for 16S rRNA gene amplicons generated 2 × 300 bp reads, and both the forward and reverse reads were demultiplexed and imported into QIIME2 (v2021.4)<sup>33</sup> (Appendix S2). The metagenomic shotgun sequencing raw data were input into the Anvi'o (v7.1) workflow and processed according to the user manual<sup>34</sup> (Appendix S3). A phylogenetic tree of reconstructed bins was constructed by comparing single-copy housekeeping genes with PhyloPhlAn 3.0.<sup>35</sup> The community composition was profiled based on database blast and the relative abundance of phylotypes following amplicon

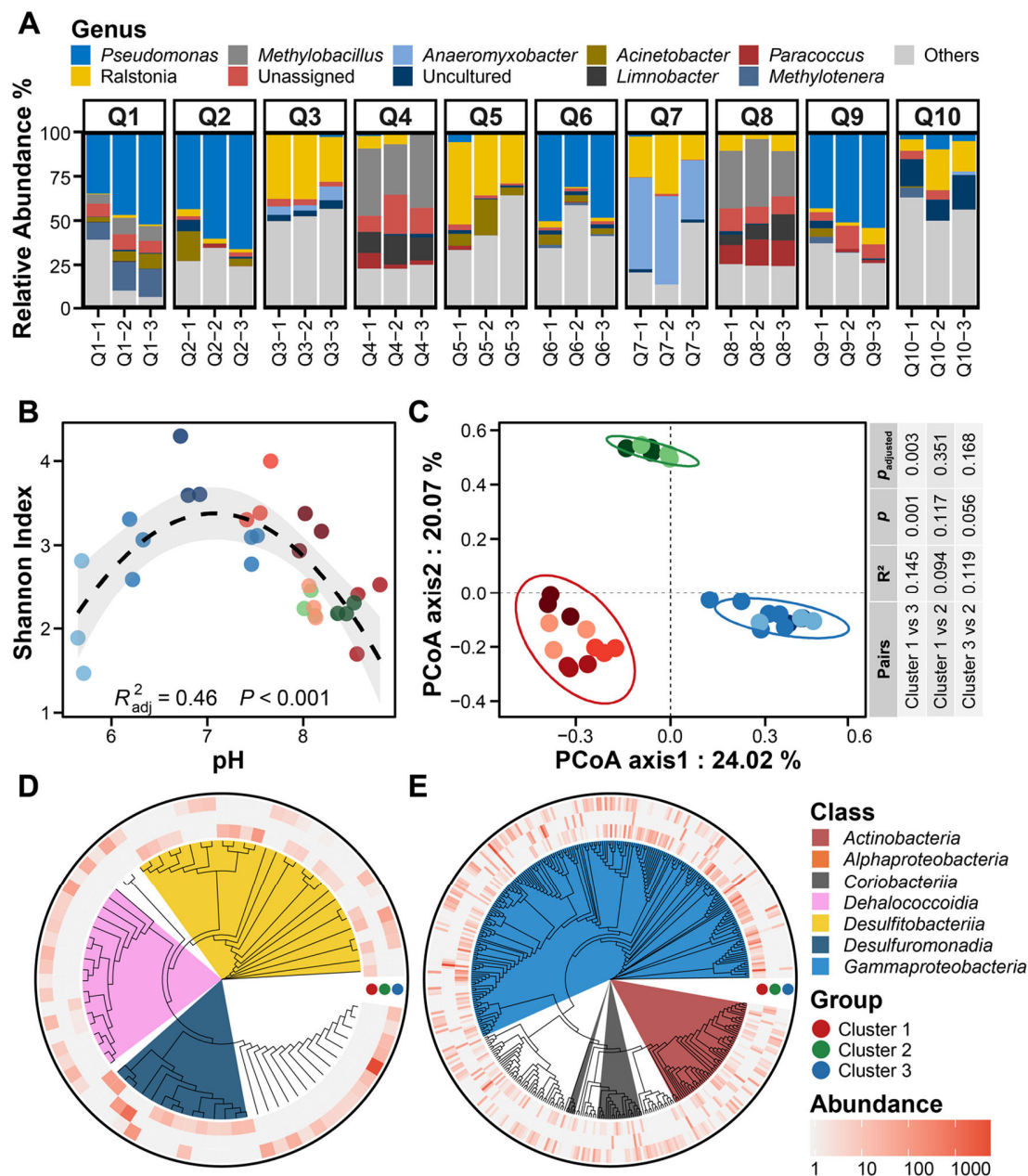


**Figure 1.** Heterogeneity of the microbial community in terms of composition and diversity. (A) Microbial community composition of each sample on genus level. (B) Quadratic regression between pH value and Shannon diversity index. (C) PCoA based on Bray–Curtis distances of the whole microbial community. Phylogenetic tree of potential degraders based on ASV feature sequences similarity for potential OHRBs (D) and BTEX degraders (E).

sequencing. Unsupervised clustering was conducted based on the Bray–Curtis distances between samples, and the distances were calculated using amplicon sequence variant (ASV) tables. The number of clusters was optimized using gap statistics.<sup>36</sup> The diversity of each sample was evaluated by computing  $\alpha$ -diversity indices in the *vegan* (v2.6–4) package<sup>37</sup> in R (v4.1.2) and QIIME2. For  $\beta$  diversity, principal coordinate analysis (PCoA) based on Bray–Curtis distances was performed using the *vegan* package to examine the differences between the soil communities in each sample (Appendix S4). Distance-based redundancy analysis (db-RDA) and variance partitioning analysis (VPA) were employed to investigate the correlations between environmental factors and the microbial community.

The *ggcor* (v0.9.8.1) and *vegan* packages were employed to conduct Spearman correlation tests and Mantel tests, respectively, based on environmental factors and the concentration of organic pollutants. The classification random forest model was constructed using the *randomForest* (v4.7–1.1) package to predict the group based on soil physiochemical factors,<sup>38</sup> while the number of remaining features was optimized using 10-fold cross-validation.

Co-occurrence relationships between ASVs in different environments were investigated by constructing a co-occurrence network separately based on the SparCC correlation<sup>39</sup> (Appendix S4). The network properties were

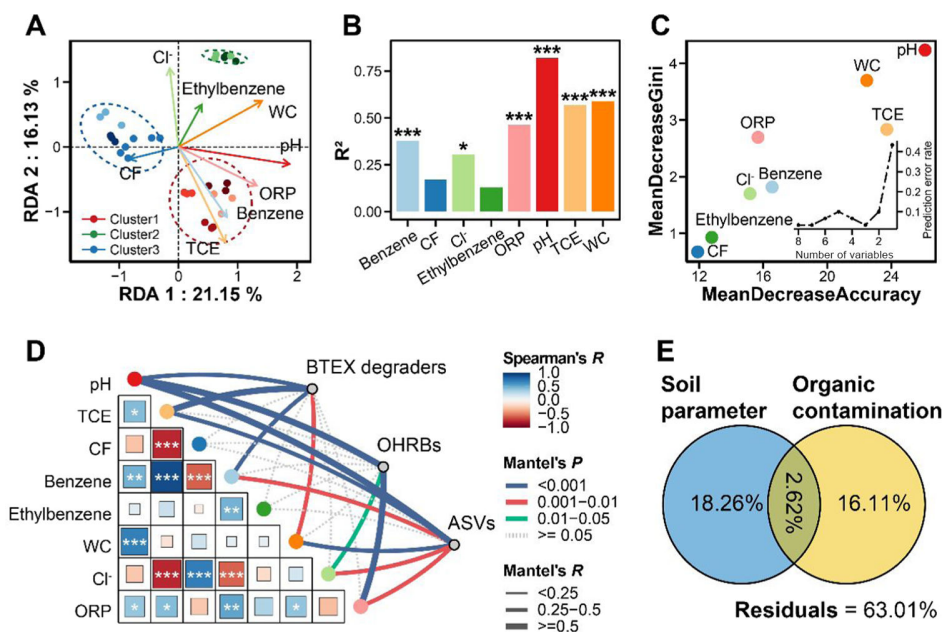


**Figure 2.** Correlation between environmental factors and microbial communities. (A) Microbial communities were constrained by environmental variables using distance-based redundancy analysis (DB-RDA; 57.58% inertia constrained). (B) db-RDA-based analysis illustrating the correlation and contribution of environmental factors to the variation of microbial communities. (C) Random forest model was constructed to predict cluster of each sample by physiochemical factors, the result indicated that pH, TCE concentration and water content were the three most important factors. (D) Spearman correlation between environmental factors and Mantel test between environmental factors and microbial community composition. (E) Variance Partitioning Analysis demonstrated the contribution of environmental characteristics (pH, water content, and Cl<sup>-</sup>) and organic cocontamination (TCE, benzene, CF, and ethylbenzene) to the variations of the microbial communities.

calculated using igraph, and the topological roles of each ASV in the network were evaluated based on ZP-plot.<sup>40</sup>

**Functional Metagenomic Profiling.** Functional annotation was conducted with hidden Markov models (HMMs) based on coding sequences (CDSs) predicted using Prodigal<sup>41</sup> in the Anvi'o workflow. These CDSs were annotated based on HMMs provided by Anvi'o, including default rRNA gene HMMs and databases, including the Kyoto Encyclopedia of Genes and Genomes (KEGG), KOfam, and Pfam. The functions related to the biodegradation of BTEX and CAHs were specifically targeted, and the fermentation capacity was also investigated (see Table S2 and Appendix S5 for details). In summary, putative reductive dehalogenases responsible for dechlorination were predicted based on HMMs retrieved from the database (TIGR02486). The oxidizing function of CAHs and their cometabolic degradation activity were characterized based on the identification of specific KEGG orthologs (KOs) and further varied with reference sequences.<sup>42</sup> The capacity for BTEX degradation was evaluated based on the completeness of relevant KEGG modules and the presence of certain genes (KOs or blast with reference sequences). Potential symbiotic species with OHRBs were identified based on the completeness of KEGG modules correlated with cofactor synthesis, acetogenesis fermentation, and hydrogen production (Appendix S6). The pH preference of each bin was predicted using a machine learning model based on the available presence/absence information for 56 selected genes, as reported previously.<sup>43</sup>

## RESULTS

**Heterogeneous Microbial Communities in the Study Area.** Triplicates of soil samples collected from 10 contaminated sample locations were analyzed for 16S rRNA

gene amplicons. Sequencing generated 1,040,720 reads (an average of 34,691 reads per sample, with a range of 22,221–49,386 reads per sample). After removing singletons and rarefying the sequencing depth to 21,000 sequences per sample, the ASV data set contained 630,000 reads and 1270 ASVs (an average of 819 reads per ASV, ranging from six to 128,725 reads). All of the samples clustered into three clusters (Cluster 1: Q1, Q2, Q6, and Q9; Cluster 2: Q4 and Q8; Cluster 3: Q3, Q5, Q7, and Q10) based on the Bray–Curtis distances of ASV composition and the gap statistic (Figure S3). Among all of the ASVs, only 21 ASVs (1.7%) were shared by all of the clusters, 437 ASVs (34.4%) were present only in Cluster 1, 70 ASVs (5.5%) were present only in Cluster 2, while 638 ASVs (50.2%) were only detected in Cluster 3 (Figure S4).

The most abundant phyla (average relative abundance >3%) included Proteobacteria (62.5 ± 22.8%), Firmicutes (11.3 ± 10.1%), Myxococcota (5.1 ± 13.7%), Bacteroidota (3.8 ± 3.5%), Patascibacteria (3.4 ± 5.7%), and Actinobacteriota (3.3 ± 2.4%) (Figure S5). Within the phylum Proteobacteria, *Gammaproteobacteria* was more abundant compared with other lineages, but its composition varied across different clusters. At the genus level, the microbial communities of Cluster 1 (Q1, Q2, Q6, and Q9) were all dominated by *Pseudomonas*. Cluster 2 (Q4 and Q8) was the only cluster with large fractions of methylotrophic *Gammaproteobacteria*, such as the genus *Methylobacillus*, whereas the genus *Ralstonia* was highly abundant in Cluster 3 (Q3, Q5, Q7, and Q10) (Figure 1A). The compositions of potential pollutant degraders, including both OHRBs (organohalide-respiring bacteria) and aromatic compound degraders, exhibited substantial diversity. Overall, obligate OHRBs and *Anaeromyxobacter* were more abundant in Cluster 3 (the relative abundance of *Dehalococcoidia* was 0.31

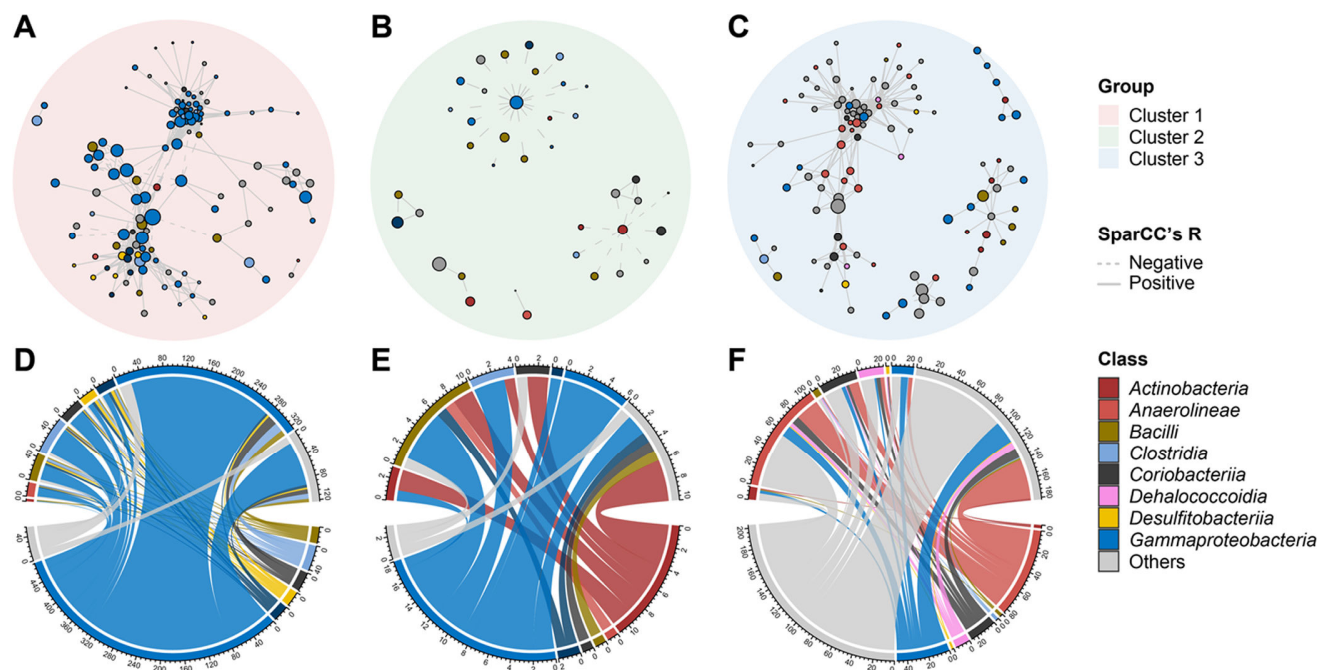


**Figure 3.** Co-occurrence networks and interclass connections. (A–C) Co-occurring networks of three clusters. (D–F) Proportion of connection between bacterial classes in the network of each cluster.

$\pm 0.53\%$ ) while *Geobacter* was enriched in Cluster 2 ( $2.88 \pm 2.00\%$ ). The abundances of *Dehalobacter* and *Desulfitobacterium* were higher in both Cluster 1 (relative abundances of  $0.72 \pm 0.53$  and  $0.24 \pm 0.44\%$ , respectively) and Cluster 3 (relative abundances of  $0.09 \pm 0.24$  and  $0.39 \pm 0.79\%$ , respectively) (Figure 1D). The diversity of BTEX degraders was greater than the diversity of OHRBs. Based on their average relative abundances, *Ralstonia* and *Pseudomonas* were more abundant in Cluster 3 and Cluster 1, respectively (Figure 1E).

The rarefaction curves tended to plateau, suggesting that the depth of the current sequencing data set was sufficient for the comparison of community diversity (Figure S6A). The only significant difference in  $\alpha$  indices was that Cluster 2 had a lower Shannon's index compared with the others (Figure S6D–F). The relationships between the pH and the Shannon's diversity index (Figure 1B;  $R_{\text{adj}}^2 = 0.46$ ,  $P < 0.001$ ), Simpson's diversity index (Figure S6B;  $R_{\text{adj}}^2 = 0.41$ ,  $P < 0.001$ ), and Pielou's evenness (Figure S6C;  $R_{\text{adj}}^2 = 0.39$ ,  $P < 0.001$ ) were described by a quadratic model. Permutational multivariate analysis of variance (PERMANOVA) illustrated that the overall differences among the communities of the three clusters were significant ( $P_{\text{adj}} < 0.001$ , Figures 1C and S7D). The Bray–Curtis distances between different clusters were also significantly higher than the distances within each cluster (Figure S7A). The composition of potential degraders also differed significantly across clusters ( $P = 0.004$  and  $P = 0.008$  for OHRBs and BTEX degraders, respectively; Figure S7).

**Correlations between Abiotic Environmental Factors and Microbiota Heterogeneity.** Environmental characteristics, including the pH, moisture content, and the concentrations of different pollutants, varied between the clusters (Figure S8). The Spearman correlation coefficient between TCE and benzene was 0.89 ( $P < 0.001$ , Figure 2D). Another unsaturated hydrocarbon, ethylbenzene, was also positively

correlated with benzene, revealing a possible co-occurrence pattern of unsaturated CAHs and BTEX. Chloroform (CF) was the predominant saturated pollutant at the site and was negatively correlated with TCE, benzene, and ethylbenzene. A positive correlation between cocontamination and pH and a negative correlation between cocontamination and water content were also observed. The random forest model and cross-validation suggested that three factors, namely, the pH, TCE concentration, and water content, contributed significantly to the differences among clusters (Figure 2C).

The Mantel test indicated that pH had the highest correlation with the microbial community ( $R_{\text{Mantel}} = 0.56$ ,  $P_{\text{Mantel}} < 0.001$ ), while TCE and benzene also associated with the community composition (TCE:  $R_{\text{Mantel}} = 0.45$ ,  $P_{\text{Mantel}} < 0.001$ ; benzene:  $R_{\text{Mantel}} = 0.35$ ,  $P_{\text{Mantel}} = 0.002$ ). From the perspective of potential function, the taxa of putative BTEX degraders were correlated with the pH, benzene content, and TCE, while putative OHRBs were also correlated with the oxidation–reduction potential in addition to the above-mentioned parameters (Figure 2C). Distance-based redundancy analysis (db-RDA) based on Bray–Curtis distances demonstrated that environmental variables explained 61.70% of the variation of the microbial community (Figure 2A). The pH was the most important parameter ( $R^2 = 0.83$ ), and cocontamination was also critical ( $R^2 = 0.62$  and  $R^2 = 0.42$  for TCE and benzene concentrations, respectively, Figure 2B). VPA indicated that environmental characteristics (pH, water content, and  $\text{Cl}^-$ ) and organic cocontamination (TCE, benzene, chloroform, and ethylbenzene) could explain 18.26 and 16.11% of the variation in the microbial community, respectively, while the combination of these two groups of factors accounted for 2.62% of the variation (Figure 2E).

**Co-Occurrence Patterns of Microbial Community.** Co-occurrence networks of the three different clusters were constructed to illustrate the differences in co-occurrence patterns under heterogeneous contaminated soil systems

(Figure 3A–C). Overall, compared with Erdős–Rényi random networks, all of the networks exhibited significantly higher modularity (MD; MD = 0.45, 0.63, and 0.40 for Clusters 1, 2, and 3, respectively; MD<sub>random</sub> = 0.24, 0.56, and 0.32, respectively), cluster coefficients (CCs; CC = 0.74, 0.07, and 0.69 for Clusters 1, 2, and 3, respectively; CC<sub>random</sub> = 0.10, 0.04, and 0.07 for Clusters 1, 2, and 3, respectively), and small-world properties ( $\sigma$ ;  $\sigma$  = 7.54, 4.70, and 13.41 for Clusters 1, 2, and 3, respectively), which reflected nonrandom microbial co-occurrence patterns in this CAH–BTEX cocontaminated soil system. Further, the degree distributions of all of the networks followed a power law, indicating that they were all scale-free networks (Figure S9A–D). Different networks were composed of different taxa. The most dominant co-occurring classes in Cluster 1 (120 ASVs) were *Gammaproteobacteria* (55 ASVs), *Clostridia* (12 ASVs), *Bacilli* (eight ASVs), *Desulfitobacteriia* (six ASVs), and *Desulfuromonadia* (six ASVs). The Cluster 2 network contained only 38 ASVs, which were affiliated with *Gammaproteobacteria* (seven ASVs), *Bacilli* (nine ASVs), *Actinobacteria* (five ASVs), *Clostridia* (four ASVs), and *Alphaproteobacteria* (six ASVs). In Cluster 3 (107 ASVs), *Anaerolineae* (17 ASVs) and *Gammaproteobacteria* (16 ASVs) were the most abundant classes, and obligate OHRBs in *Dehalococcoidia* (three ASVs) were also observed. ASVs observed in all of the networks were classified as peripherals, network connectors, module hubs, or network hubs based on their within-module connectivity ( $Z_i$ ) and among-module connectivity ( $P_i$ ).

In Clusters 1 and 2, most keystone ASVs (module hubs, network hubs, and connectors) were affiliated with *Gammaproteobacteria* (Figure S9D–F). In Cluster 3, network connectors contained a high proportion of ASVs from *Anaerolineae* and *Dehalococcoidia*. In addition, the connection between classes differed (Figure 3D–F). The majority of the connections were between different *Gammaproteobacteria* in Clusters 1 and 2, while in Cluster 3, connections within *Anaerolineae* and connections between *Anaerolineae* and *Gammaproteobacteria* were more common. OHRBs in Cluster 3 were linked with other OHRBs or *Anaerolineae* and *Coriobacteriia*, which suggests that these lineages may be involved in reductive dechlorination.

**Metagenomic Insight into Microbial Community Functions.** Overall, metagenomic sequencing generated 90 Gb of raw data with 30 Gb per site in total. After quality control, 273,267,162 clean reads remained and were assembled into 298,998 contigs with lengths of over 1 kb. In total, 935,298 genes were predicted from these contigs. A total of 182 bins were recovered, which represented 79.41% of the sequenced nucleotides. Among these bins, 14, 40, and 58 bins were qualified as high-, medium-, and low-quality metagenome-assembled genomes (MAGs), respectively (Appendix S3 and Table S3), while the rest of bins with contamination higher than 10% were merely regarded as a cluster of similar contigs. Both MAGs and bins were used for further analysis. Taxonomic annotation suggested that 63 MAGs and 29 bins were affiliated with Firmicutes, including potential OHRBs (*Desulfotomaculia* and *Desulfitobacteriia*). Proteobacteria was also extensively recovered from the metagenomic sequencing data set, including 18 MAGs and 21 bins. In addition, 15 MAGs and nine bins were affiliated with Actinobacteriota (Table S2).

A total of nine putative reductive dehalogenases were identified in the metagenomic data set and were found in six

bins (Table S3 and Figure S10). Taxonomically, these putative OHRB bins were affiliated with taxa including *Negativicutes*, *Clostridia*, *Bacilli*, and *Dehalobacteriia* at the class level (Figures 4 and S10). The MAGs and bins with genes related to

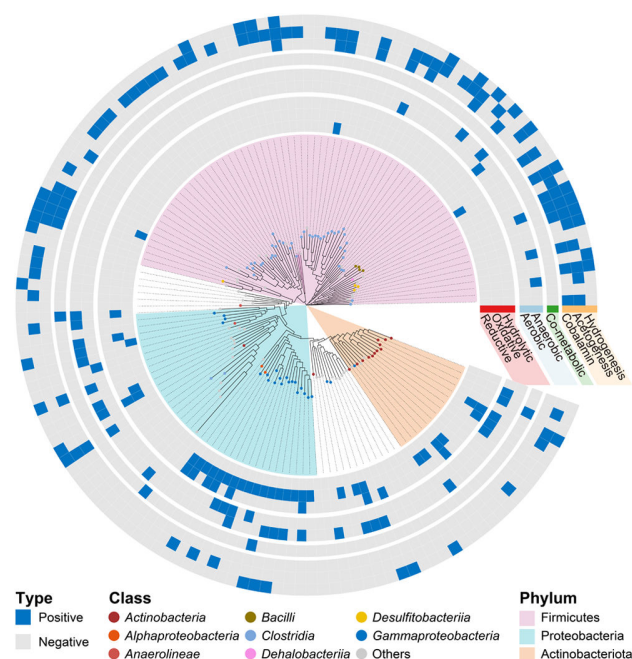


**Figure 4.** Functional profiling of MAGs. Phylogeny of reconstructed MAGs. Maximum-likelihood tree of concatenated amino acid sequences of conserved single copy genes (SCGs). Taxonomy was labeled by point on class level while on phylum level, Firmicutes, Proteobacteria, and Actinobacteriota clade were colored in the sector. Heatmaps demonstrate the presence of biodegradation-related functions in each bin. Bins with inadequate SCGs were not covered in this tree.

cobalamin, hydrogen, and acetate production were also investigated due to their potential roles in promoting the bacterial activity of reductive dechlorination (Figure 5). Twenty-seven bins were identified as cobalamin-producing syntrophic members with relatively complete cobalamin *de novo* synthesis functions (Figure 4 and Table S5). The majority of these bins (24 of 27 bins) were affiliated with Firmicutes (on the class level, *Desulfitobacteriia*, *Desulfotomaculia*, *Dehalobacteriia*, *Syntrophomonadia*, *Negativicutes*, *Bacilli*, and *Clostridia*), while *Synergistota* and Actinobacteriota can also produce cofactors (Figure 4 and Table S4). Most of the above-mentioned taxa were also predicted to produce hydrogen and acetate via the fermentation of metabolites from organic pollutants (Figure 4 and Tables S6 and S7). For oxidative CAH-degrading pathways, epoxyalkane:coenzyme M transferase (EaCoMT) was only detected in two  $\gamma$ -Proteobacteria bins (BIN-162 and MAG-M054; Table S10 and Figures 4 and S8). Hydrolytic dechlorination functions, haloalkane dehalogenase and haloacetate dehalogenase, were mainly observed in Proteobacteria and Actinobacteriota (Figure 4 and Table S10). In addition, glutathione S-transferase (GST), which can inactivate electrophilic substrates, was widely detected in bins affiliated with Proteobacteria and Actinobacteriota. Three bins affiliated with  $\gamma$ -Proteobacteria (two of these bins were *Pseudomonas*) contained as many as 21, 20, and 14 copies of GST, while other Proteobacteria lineages, including *Methyl-*

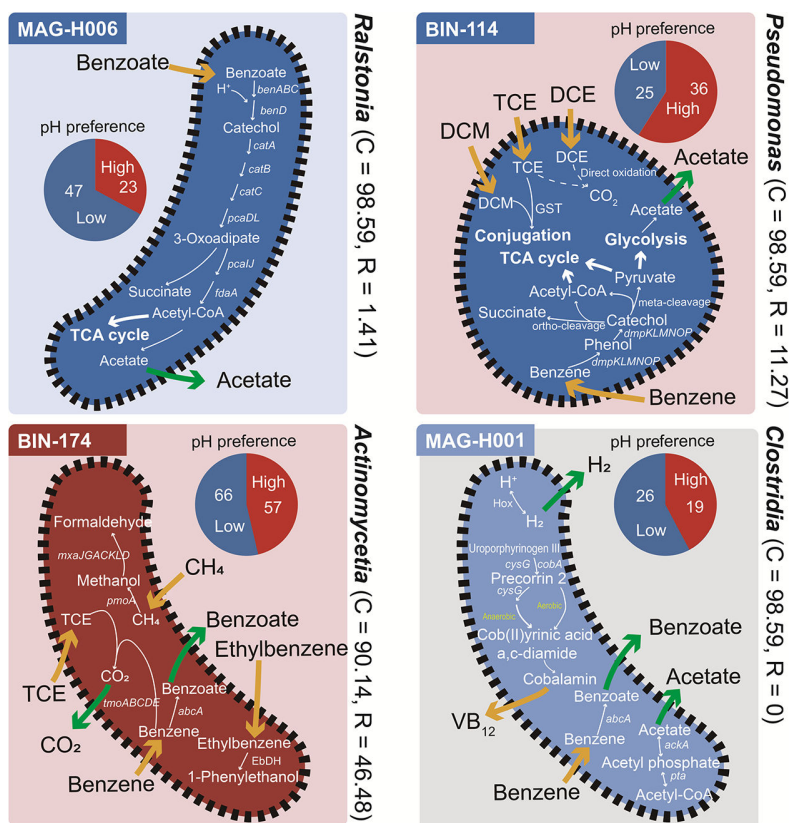


**Figure 5.** Pathways involved in organic pollutant degradation, fermentation, and pH preference of representative MAGs. Metabolic potential of representative MAGs/bins of dominant bacteria *Ralstonia* and *Pseudomonas*. The amount of previously reported pH preference-related genes in each MAG/bin were shown in the pie chart.

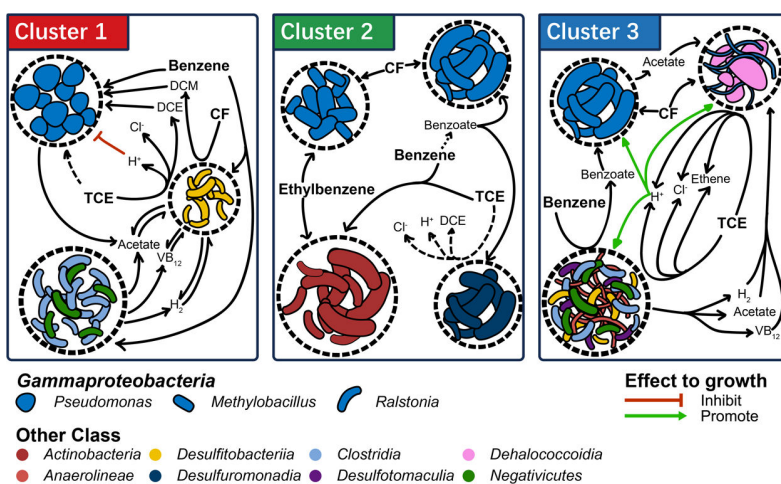


**Figure 6.** Hypothetical schematic diagram of microbial degradation in different bacterial clusters. Significant interactions between major bacterial clades and biodegradation processes are indicated by lines in the diagram. Solid lines represent potential metabolic pathways annotated based on metagenomic bins. Conversely, dashed lines signify functions that, despite extensive reports in prior literature, were not detected within our metagenomic binning data set.

*obacillus*, *Anaeromyxobacter*, and *Sulfurifustis*, also contained GST genes (Figure 4 and Table S10).

Only three bins (BIN-114, BIN-150, and BIN-163) contained genes encoding enzymes for converting the predominant pollutant, benzene, into catechol. These bins were all affiliated with *Pseudomonas*; therefore, they were the only possible aerobic benzene degraders identified at this site (Figure 4 and Table S8). Potential xylene and toluene

biodegradation functions were observed in both Proteobacteria and Actinobacteriota. In contrast, microorganisms with anaerobic BTEX degradation functions were more diverse, including bins affiliated with Proteobacteria (13 bins), Firmicutes (seven bins), Desulfobacterota (three bins), and Cyanobacteria (three bins) (Figure 4 and Table S9). Among these bins, five Firmicutes, three Desulfobacterota, three Proteobacteria, and one Cyanobacteria bin carried the *abcA*

gene. These taxa were also potential hosts of anaerobic ethylbenzene and anaerobic toluene degradation functions. Two Firmicutes bins (BIN-146 and BIN-156) were predicted to contain benzylsuccinate synthase genes. Genes encoding anaerobic ethylbenzene dehydrogenase were present in bins affiliated with Proteobacteria (11 bins) and other taxa, including Actinobacteriota (one bin) and Cyanobacteria (two bins). Therefore, they were considered capable of the anaerobic degradation of toluene and ethylbenzene. Genes coding for methane/ammonia monooxygenase were detected in MAGs of Actinobacteriota, Thermoproteota, and Proteobacteria. These MAGs, together with other monooxygenases containing MAGs, were believed to cometabolically degrade CAH and BTEX simultaneously.

The genomic features of the dominant *Gammaproteobacteria* lineages varied significantly. *Ralstonia* was more strongly correlated with a lower pH environment, while *Pseudomonas* was correlated with higher pH levels. The *Ralstonia* MAG contained benzoate-degrading genes, while the *Pseudomonas* MAG contained more oxygenase genes and a higher number of GST copies. *Methylobacillus*, another dominant genus in Cluster 2, contained genes associated with the anaerobic degradation of benzene and ethylbenzene degradation. These functional genes were also widely observed in *Actinomyces* bins. In addition, hydrogen-producing, acetate-producing, and cofactor-synthesizing genes were found in dominant *Clostridia* bins (Figure 5).

## DISCUSSION

In this study, samples collected from 10 sampling locations in an area of 20 m by 20 m at a BTEX–CAH cocontaminated site were categorized into three distinct clusters based on their microbial community composition. The limited numbers of shared ASVs and their overall low occupancy among the samples demonstrated a high heterogeneity of indigenous microbial communities. Taxonomical profiling indicated that different lineages within the dominant phylum, Proteobacteria, were enriched in each cluster (*Pseudomonas*, *Methylobacillus*, and *Ralstonia* in Clusters 1, 2, and 3, respectively, Figure 6). Bray–Curtis distance-based  $\beta$ -diversity analysis indicated that the three clusters displayed significant compositional variance. This difference was attributed to specific environmental factors. Overall, the pH level and cocontamination with TCE and benzene had the strongest correlation with the community compositions. The potential roles of these factors as driving factors for the formation of different clusters among samples were consistent with previous reports.<sup>44</sup> In addition, the abundance and composition of potential degraders for various pollutants varied significantly across different clusters (Figures 1D and S7). Although this analysis was based on putative degraders predicted using taxonomic information (Appendix S4), such significant differences were still noteworthy as the degrading functional genes and pathways were further confirmed by metagenomic binning results.

Samples from Cluster 1 were characterized by high pH values and elevated concentrations of TCE and benzene (Figure S8). It is hypothesized that these environmental factors shape the observed community composition by favoring microbes that demonstrate high tolerance to contamination and a preference for elevated pH values. The dominance of *Pseudomonas* was most likely driven by the presence of multiple copies of benzene-degrading genes and genes encoding GST, as well as various proteins that have been predicted to be

associated with a high pH preference.<sup>44</sup> It has been documented that GST effectively promotes the oxidation and detoxification of CAHs by conjugating with glutathione,<sup>16</sup> thereby enhancing the resilience and adaptability of *Pseudomonas* under severely polluted environments. The ability to utilize benzene and the preference for high pH further promoted the growth of *Pseudomonas* in this cluster. Regarding OHRBs, the dominance of *Dehalobacter* over obligate OHRBs could be explained by the growth rate–yield theory. Some OHRBs, such as *Dehalobacter*, grow rapidly when sufficient CAHs are available.<sup>45–46,47</sup> However, their biomass diminished more rapidly following substrate removal compared to *Dehalococcoides*. This could be attributed to disparities in their resistance to unfavorable growth conditions or differences in their capacity to metabolize substrates at varying concentrations.<sup>45</sup> In conclusion, the results indicated that pH preference and substrate concentration were the primary factors contributing to the predominance of *Dehalobacter* and *Pseudomonas* in the Cluster 1 samples.

In Cluster 2 samples, the genus *Methylobacillus*, another *Gammaproteobacteria*, was the most dominant member, different from the dominance of *Pseudomonas* in Cluster 1. This was suspected to be the result of a high concentration of one-carbon substrate in Cluster 2 samples. A large proportion of *Actinobacteria* was also observed in Cluster 2 samples. Some metagenomic binning MAGs affiliated with this class were also predicted to harbor methane/ammonia monooxygenases. These enzymes could potentially catalyze the cometabolization of TCE.<sup>16,24,25</sup> Notably, within the dominant classes *Gammaproteobacteria* and *Actinobacteria*, genera such as *Microbacterium* and *Methylobacillus* were found to harbor functional genes encoding core enzymes responsible for the initial oxygenation step in ethylbenzene and benzene degradation pathways. Besides, sequential benzoate degradation genes were detected in the *Ralstonia* MAGs. Therefore, collaborations among different bacteria might play an important role in the biodegradation of BTEX in these samples.

The high abundance of obligate OHRBs in Cluster 3 samples was consistent with these soil samples being potential hotspots of reductive dechlorination. Low CAH concentrations together with high levels of chloride ions in these soil samples supported this hypothesis. Genes associated with the de novo synthesis of vitamin B<sub>12</sub> were detected in the MAGs of *Ralstonia*, which was highly dominant in Cluster 3 (and present in other clusters). These genes were also detected in *Clostridia* MAGs. Both *Ralstonia* and *Clostridia* may serve as cooperative microbes by supplying cofactors to OHRB RDase. Correlations between OHRBs and ASVs annotated as *Anaerolineaceae* were also observed in the Cluster 3 co-occurrence network. Previous studies have shown that multiple *Anaerolineaceae* are fermentative microorganisms.<sup>48,49</sup> Moreover, these *Anaerolineaceae* have been widely observed to co-occur with obligate OHRBs under CAH-contaminated conditions.<sup>50–52</sup> Based on the predominant degrading genes in Cluster 3, it is hypothesized that benzene is likely to be anaerobically degraded to benzoate by *Clostridia* members and this intermediate can be degraded by *Ralstonia* and converted into fatty acids to enhance cofactor production.<sup>9</sup> Under low CAH concentrations, given sufficient critical cofactors and an appropriate growth rate/yield trade-off, obligate OHRBs are expected to be enriched. Coexistence with *Ralstonia*, *Clostridia*, and *Anaerolineaceae* facilitated the degradation of CAHs by



providing fermentation products and cofactors to OHRBs in Cluster 3 samples. Numerous pollutants tend to be degraded through multiple pathways depending on the local environment, microbial communities, and the chemical nature of the pollutants.<sup>9,15,26</sup> CAHs and BTEX, common organic pollutants, often co-occur at industrial sites. These compounds can be degraded by both aerobic and anaerobic bacteria. However, the preferred biodegradation mechanisms and pathways of these compounds in highly heterogeneous industrial contaminated sites and the spatial-scale distribution among different possible pathways have not been evaluated. In the present study, a comprehensive analysis of the physicochemical parameters and microbiome revealed that a site contaminated with both CAHs and BTEX presented significant variations in both the microbial communities and pollutant-degrading members over a scale of meters. The spatial distributions of organic pollutants affected the community composition and diversity, co-occurrence patterns, and degrading functions. The indigenous microbial communities were enriched spatially in various small-scale ecological niches, potentially temporally, which is to be evaluated in future studies.

Previous studies have introduced targeted bioremediation approaches utilizing site-level metagenomics to enhance remediation efficacy.<sup>28</sup> Building on this foundation, we propose refining existing frameworks by investigating the smaller-scale heterogeneity of contaminated sites and optimizing bioremediation at the microbial community level. Unlike traditional contamination-centric methods, which primarily focus on the distribution of pollutants, our community-oriented strategy also emphasizes in situ distribution of microbiome. This is especially crucial for optimizing the bioremediation in complex cocontaminated environments.

This approach integrates three essential components: site-specific geochemical parameters, functional characterization of degraders and syntrophic consortia, and microbial co-occurrence patterns. While recent advancements emphasize managing environmental heterogeneity (e.g., Wu et al.'s bioaugmentation using niche-modifying cultures to create methanogenic zones<sup>53</sup>), such strategies face challenges in cocontaminated systems where conflicting redox requirements emerge. Low ORP inhibits BTEX degradation while oxygenation stresses OHRBs. Our methodology overcomes these limitations by avoiding nonphysiologically optimal conditions across diverse contaminated sites. This is achieved by (1) identifying preferential contaminant removal routes and (2) mapping cross-pollutant interaction dynamics, enabling customized solutions. For instance, Wu's approach would succeed in sites dominated by Cluster 3 consortia containing abundant OHRBs, whereas oxygen-amended approaches would demonstrate superior remediation outcomes in Clusters 1 and 2 predominant environments.

Ultimately, understanding indigenous microbial responses to multipollutant stress is pivotal for developing optimized bioremediation protocols. Our work emphasizes the significance of discerning community patterns, characterizing their functional roles, and reconstructing metabolic models. This innovative precision framework has the potential to enhance in situ remediation efficacy at heterogeneous sites, offering scalable solutions for global contamination challenges.

## ■ ASSOCIATED CONTENT

### Supporting Information

The Supporting Information is available free of charge at <https://pubs.acs.org/doi/10.1021/acs.est.4c10071>.

Additional experimental details, materials, and methods, including preincubation of low biomass samples; process of sequencing data, summary of methods and statistical analysis; list of bins recovered from the metagenomic data; summary of functional genes and their presence in the MAGs; overview of field sampling design; physicochemical parameters of each site; unsupervised clustering of samples; distribution of ASVs in amplicon sequencing data; community composition of each site at the phylum level; comparison of community diversity; topology of co-occurrence networks; and verification of functional gene annotations (PDF)

## ■ AUTHOR INFORMATION

### Corresponding Author

**Xiaojun Zhang** – State Key Laboratory of Microbial Metabolism, Joint International Research Laboratory of Metabolic & Developmental Sciences, and School of Life Sciences & Biotechnology, Shanghai Jiao Tong University, Shanghai 200240, China; [orcid.org/0000-0002-4559-0177](https://orcid.org/0000-0002-4559-0177); Phone: +86 21-34204878; Email: [xjzhang68@sjtu.edu.cn](mailto:xjzhang68@sjtu.edu.cn)

### Authors

**Kaiwen Yang** – State Key Laboratory of Microbial Metabolism, Joint International Research Laboratory of Metabolic & Developmental Sciences, and School of Life Sciences & Biotechnology, Shanghai Jiao Tong University, Shanghai 200240, China

**Lei Zhang** – State Key Laboratory of Microbial Metabolism, Joint International Research Laboratory of Metabolic & Developmental Sciences, and School of Life Sciences & Biotechnology, Shanghai Jiao Tong University, Shanghai 200240, China

**Azariel Ruiz-Valencia** – Laboratoire d'Ecologie Microbienne, UMR CNRS 5557, UMR INRAE 418, VetAgro Sup, Université Claude Bernard Lyon 1, Villeurbanne 69622, France; [orcid.org/0000-0002-6948-6593](https://orcid.org/0000-0002-6948-6593)

**Xin Song** – State Key Laboratory of Soil and Sustainable Agriculture, Institute of Soil Science, Chinese Academy of Sciences, Nanjing 211135, China; [orcid.org/0000-0001-7655-4497](https://orcid.org/0000-0001-7655-4497)

**Timothy M. Vogel** – Laboratoire d'Ecologie Microbienne, UMR CNRS 5557, UMR INRAE 418, VetAgro Sup, Université Claude Bernard Lyon 1, Villeurbanne 69622, France

Complete contact information is available at: <https://pubs.acs.org/doi/10.1021/acs.est.4c10071>

### Author Contributions

K.Y.: Conceptualization, methodology, data analysis and writing the original draft. L.Z.: Methodology and enrichment experiment. A.R.V.: Methodology and data analysis. X.S.: Field selection, field data, funding acquisition, manuscript editing. T.M.V.: Data analysis and manuscript writing and editing. X.Z.: Conceptualization, investigation, writing—review and editing, supervision, and funding acquisition.

## Notes

The authors declare no competing financial interest.

## ACKNOWLEDGMENTS

This work was supported by the National Natural Science Foundation of China (Project 32061133001). We acknowledge the cooperation between China and the EU through the EiCLaR project (European Union's Horizon 2020, N°965945). We thank LetPub for its linguistic assistance.

## REFERENCES

- (1) Maji, S.; Beig, G.; Yadav, R. Winter VOCs and OVOCs measured with PTR-MS at an urban site of India: Role of emissions, meteorology and photochemical sources. *Environ. Pollut.* **2020**, *258*, No. 113651.
- (2) Tehrani, A. M.; Bahrami, A.; Leili, M.; Poorolajal, J.; Zafari, D.; Samadi, M.; Mahvi, A. H. Investigation of seasonal variation and probabilistic risk assessment of BTEX emission in municipal solid waste transfer station. *Int. J. Environ. Anal. Chem.* **2022**, *102* (18), 6626–6639.
- (3) Kansal, A. Sources and reactivity of NMHCs and VOCs in the atmosphere: A review. *J. Hazard. Mater.* **2009**, *166* (1), 17–26.
- (4) Demirel, G.; Ozden, O.; Dogeroglu, T.; Gaga, E. O. Personal exposure of primary school children to BTEX, NO<sub>2</sub> and ozone in Eskisehir, Turkey: Relationship with indoor/outdoor concentrations and risk assessment. *Sci. Total Environ.* **2014**, *473–474*, 537–548.
- (5) Bassig, B. A.; Zhang, L.; Vermeulen, R.; Tang, X.; Li, G.; Hu, W.; Guo, W.; Purdue, M. P.; Yin, S.; Rappaport, S. M.; Shen, M.; Ji, Z.; Qiu, C.; Ge, Y.; Hosgood, H. D.; Reiss, B.; Wu, B.; Xie, Y.; Li, L.; Yue, F.; Freeman, L. E. B.; Blair, A.; Hayes, R. B.; Huang, H.; Smith, M. T.; Rothman, N.; Lan, Q. Comparison of hematological alterations and markers of B-cell activation in workers exposed to benzene, formaldehyde and trichloroethylene. *Carcinogenesis* **2016**, *37* (7), 692–700.
- (6) EPA. U. S. Priority Pollutant List, 40 CFR Part 423, 2014.
- (7) Shim, H. J.; Ma, W.; Lin, A. J.; Chan, K. C. Bio-removal of mixture of benzene, toluene, ethylbenzene, and xylenes/total petroleum hydrocarbons/trichloroethylene from contaminated water. *J. Environ. Sci.* **2009**, *21* (6), 758–763.
- (8) Chen, L.; Liu, Y. L.; Liu, F.; Jin, S. Treatment of co-mingled benzene, toluene and TCE in groundwater. *J. Hazard. Mater.* **2014**, *275*, 116–120.
- (9) Zhang, X.; Luo, M.; Deng, S.; Long, T.; Sun, L.; Yu, R. Field study of microbial community structure and dechlorination activity in a multi-solvents co-contaminated site undergoing natural attenuation. *J. Hazard. Mater.* **2022**, *423*, No. 127010.
- (10) Wang, Q.; Guo, S.; Ali, M.; Song, X.; Tang, Z.; Zhang, Z.; Zhang, M.; Luo, Y. Thermally enhanced bioremediation: A review of the fundamentals and applications in soil and groundwater remediation. *J. Hazard. Mater.* **2022**, *433*, No. 128749.
- (11) Ghandehari, S. S.; Boyer, J.; Ronin, D.; White, J. R.; Hapeman, C. J.; Jackson, D.; Kaya, D.; Torrents, A.; Kjellerup, B. V. Use of organic amendments derived from biosolids for groundwater remediation of TCE. *Chemosphere* **2023**, *323*, No. 138059.
- (12) Tiehm, A.; Schmidt, K. R. Sequential anaerobic/aerobic biodegradation of chloroethenes—aspects of field application. *Curr. Opin. Biotechnol.* **2011**, *22* (3), 415–421.
- (13) Jugder, B. E.; Ertan, H.; Bohl, S.; Lee, M.; Marquis, C. P.; Manefield, M. Organohalide Respiring Bacteria and Reductive Dehalogenases: Key Tools in Organohalide Bioremediation. *Front. Microbiol.* **2016**, *7*, No. 249.
- (14) Hermon, L.; Hellal, J.; Denonfoux, J.; Vuilleumier, S.; Imfeld, G.; Urien, C.; Ferreira, S.; Joulain, C. Functional Genes and Bacterial Communities During Organohalide Respiration of Chloroethenes in Microcosms of Multi-Contaminated Groundwater. *Front. Microbiol.* **2019**, *10*, No. 89.
- (15) Gaza, S.; Schmidt, K. R.; Weigold, P.; Heidinger, M.; Tiehm, A. Aerobic metabolic trichloroethene biodegradation under field-relevant conditions. *Water Res.* **2019**, *151*, 343–348.
- (16) Xing, Z.; Su, X.; Zhang, X.; Zhang, L.; Zhao, T. Direct aerobic oxidation (DAO) of chlorinated aliphatic hydrocarbons: A review of key DAO bacteria, biometabolic pathways and *in-situ* bioremediation potential. *Environ. Int.* **2022**, *162*, No. 107165.
- (17) Liu, X.; Timothy, E. M. Epoxyalkane:Coenzyme M Transferase Gene Diversity and Distribution in Groundwater Samples from Chlorinated-Ethene-Contaminated Sites. *Appl. Environ. Microb.* **2016**, *82* (11), 3269–3279.
- (18) Banerjee, S.; Bedics, A.; Toth, E.; Kriszt, B.; Soares, A. R.; Boka, K.; Tancsics, A. Isolation of *Pseudomonas aromaticivorans* sp. nov from a hydrocarbon-contaminated groundwater capable of degrading benzene-, toluene-, m- and p-xylene under microaerobic conditions. *Front. Microbiol.* **2022**, *13*, No. 929128, DOI: 10.3389/fmicb.2022.929128.
- (19) Huizenga, J. M.; Semprini, L. Influence of growth substrate and contaminant mixtures on the degradation of BTEX and MTBE by *Rhodococcus rhodochrous* ATCC strain 21198. *Biodegradation* **2023**, *34* (5), 461–475.
- (20) Toth, C. R. A.; Luo, F.; Bawa, N.; Webb, J.; Guo, S.; Dworatzek, S.; Edwards, E. A. Anaerobic Benzene Biodegradation Linked to the Growth of Highly Specific Bacterial Clades. *Environ. Sci. Technol.* **2021**, *55* (12), 7970–7980.
- (21) Lueders, T. The ecology of anaerobic degraders of BTEX hydrocarbons in aquifers. *FEMS Microbiol. Ecol.* **2017**, *93* (1), No. fiv220.
- (22) Li, J.; de Toledo, R. A.; Chung, J.; Shim, H. Removal of mixture of cis-1,2-dichloroethylene/trichloroethylene/benzene, toluene, ethylbenzene, and xylenes from contaminated soil by *Pseudomonas plecoglossicida*. *J. Chem. Technol. Biotechnol.* **2014**, *89* (12), 1934–1940.
- (23) Ryoo, D.; Shim, H.; Canada, K.; Barbieri, P.; Wood, T. K. Aerobic degradation of tetrachloroethylene by toluene-o-xylene monooxygenase of *Pseudomonas stutzeri* OX1. *Nat. Biotechnol.* **2000**, *18* (7), 775–778.
- (24) Shao, Y.; Hatzinger, P. B.; Streger, S. H.; Rezes, R. T.; Chu, K. H. Evaluation of methanotrophic bacterial communities capable of biodegrading trichloroethene (TCE) in acidic aquifers. *Biodegradation* **2019**, *30* (2–3), 173–190.
- (25) Shukla, A. K.; Vishwakarma, P.; Upadhyay, S. N.; Tripathi, A. K.; Prasana, H. C.; Dubey, S. K. Biodegradation of trichloroethylene (TCE) by methanotrophic community. *Bioresour. Technol.* **2009**, *100* (9), 2469–2474.
- (26) Gafni, A.; Siebner, H.; Bernstein, A. Potential for co-metabolic oxidation of TCE and evidence for its occurrence in a large-scale aquifer survey. *Water Res.* **2020**, *171*, No. 115431.
- (27) Elango, V.; Kurtz, H. D.; Freedman, D. L. Aerobic cometabolism of trichloroethene and cis-dichloroethene with benzene and chlorinated benzenes as growth substrates. *Chemosphere*. **2011**, *84* (2), 247–253.
- (28) Redfern, L. K.; Gardner, C. M.; Hodzic, E.; Ferguson, P. L.; Hsu-Kim, H.; Gunsch, C. K. A new framework for approaching precision bioremediation of PAH contaminated soils. *J. Hazard. Mater.* **2019**, *378*, No. 120859.
- (29) Nunan, N.; Schmidt, H.; Raynaud, X. The ecology of heterogeneity: soil bacterial communities and C dynamics. *Philos. Trans. R. Soc., B* **2020**, *375* (1798), No. 20190249.
- (30) Thijs, S.; de Beeck, M. O.; Beckers, B.; Truyens, S.; Stevens, V.; van Hamme, J. D.; Weyens, N.; Vangronsveld, J. Comparative Evaluation of Four Bacteria-Specific Primer Pairs for 16S rRNA Gene Surveys. *Front. Microbiol.* **2017**, *8*, No. 494.
- (31) Qin, X. C.; Wu, X. G.; Li, L. F.; Li, C. J.; Zhang, Z. J.; Zhang, X. J. The Advanced Anaerobic Expanded Granular Sludge Bed (AnaEG) Possessed Temporally and Spatially Stable Treatment Performance and Microbial Community in Treating Starch Processing Wastewater. *Front. Microbiol.* **2018**, *9*, No. 589.

- (32) Löffler, F. E.; Sanford, R. A.; Ritalahti, K. M. Enrichment, Cultivation, and Detection of Reductively Dechlorinating Bacteria. In *Methods in Enzymology*; Elsevier, 2005; Vol. 397, pp 77–111.
- (33) Bolyen, E.; Rideout, J. R.; Dillon, M. R.; Bokulich, N.; Abnet, C. C.; Al-Ghalith, G. A.; Alexander, H.; Alm, E. J.; Arumugam, M.; Asnicar, F.; Bai, Y.; Bisanz, J. E.; Bittinger, K.; Brejnrod, A.; Brislawn, C. J.; Brown, C. T.; Callahan, B. J.; Caraballo-Rodriguez, A. M.; Chase, J.; Cope, E. K.; da Silva, R.; Diener, C.; Dorrestein, P. C.; Douglas, G. M.; Durall, D. M.; Duvallet, C.; Edwardson, C. F.; Ernst, M.; Estaki, M.; Fouquier, J.; Gauglitz, J. M.; Gibbons, S. M.; Gibson, D. L.; Gonzalez, A.; Gorlick, K.; Guo, J. R.; Hillmann, B.; Holmes, S.; Holste, H.; Huttenhower, C.; Huttley, G. A.; Janssen, S.; Jarmusch, A. K.; Jiang, L. J.; Kaehler, B. D.; Kang, K. B.; Keefe, C. R.; Keim, P.; Kelley, S. T.; Knights, D.; Koester, I.; Kosciulek, T.; Kreps, J.; Langille, M. G. I.; Lee, J.; Ley, R.; Liu, Y. X.; Loftfield, E.; Lozupone, C.; Maher, M.; Marotz, C.; Martin, B. D.; McDonald, D.; McIver, L. J.; Melnik, A. V.; Metcalf, J. L.; Morgan, S. C.; Morton, J. T.; Naimey, A. T.; Navas-Molina, J. A.; Nothias, L. F.; Orchanian, S. B.; Pearson, T.; Peoples, S. L.; Petras, D.; Preuss, M. L.; Pruesse, E.; Rasmussen, L. B.; Rivers, A.; Robeson, M. S.; Rosenthal, P.; Segata, N.; Shaffer, M.; Shiffer, A.; Sinha, R.; Song, S. J.; Spear, J. R.; Swafford, A. D.; Thompson, L. R.; Torres, P. J.; Trinh, P.; Tripathi, A.; Turnbaugh, P. J.; Ul-Hasan, S.; vander Hoof, J. J. J.; Vargas, F.; Vazquez-Baeza, Y.; Vogtmann, E.; von Hippel, M.; Walters, W.; Wan, Y. H.; Wang, M. X.; Warren, J.; Weber, K. C.; Williamson, C. H. D.; Willis, A. D.; Xu, Z. Z.; Zaneveld, J. R.; Zhang, Y. L.; Zhu, Q. Y.; Knight, R.; Caporaso, J. G. Reproducible, interactive, scalable and extensible microbiome data science using QIIME 2. *Nat. Biotechnol.* **2019**, *37* (8), 852–857.
- (34) Eren, A. M.; Esen, Ö. C.; Quince, C.; Vineis, J. H.; Morrison, H. G.; Sogin, M. L.; Delmont, T. O. Anvi'o: an advanced analysis and visualization platform for 'omics data. *PeerJ* **2015**, *3*, No. e1319.
- (35) Asnicar, F.; Thomas, A. M.; Beghini, F.; Mengoni, C.; Manara, S.; Manghi, P.; Zhu, Q.; Bolzan, M.; Cumbo, F.; May, U.; Sanders, J. G.; Zolfo, M.; Kopylova, E.; Pasolli, E.; Knight, R.; Mirarab, S.; Huttenhower, C.; Segata, N. Precise phylogenetic analysis of microbial isolates and genomes from metagenomes using PhyloPhlAn 3.0. *Nat. Commun.* **2020**, *11* (1), No. 2500.
- (36) Tibshirani, R.; Walther, G.; Hastie, T. Estimating the Number of Clusters in a Data Set Via the Gap Statistic. *J. R. Stat. Soc. Ser. B: Stat. Methodol.* **2001**, *63* (2), 411–423.
- (37) Dixon, P. VEGAN, a package of R functions for community ecology. *J. Veg. Sci.* **2003**, *14* (6), 927–930.
- (38) Liaw, A.; Wiener, M. Classification and regression by randomForest. *R News* **2002**, *2* (3), 18–22.
- (39) Friedman, J.; Alm, E. J. Inferring correlation networks from genomic survey data. *PLoS Comput. Biol.* **2012**, *8* (9), No. e1002687.
- (40) Tu, Q.; Yan, Q.; Deng, Y.; Michaletz, S. T.; Buzzard, V.; Weiser, M. D.; Waide, R.; Ning, D.; Wu, L.; He, Z.; Zhou, J. Biogeographic patterns of microbial co-occurrence ecological networks in six American forests. *Soil Biol. Biochem.* **2020**, *148*, No. 107897.
- (41) Hyatt, D.; Chen, G. L.; Locascio, P. F.; Land, M. L.; Larimer, F. W.; Hauser, L. J. Prodigal: prokaryotic gene recognition and translation initiation site identification. *BMC Bioinf.* **2010**, *11*, No. 119.
- (42) Lee, J. Y.; Choi, M.; Song, M. J.; Kim, D. D.; Yun, T.; Chang, J.; Ho, A.; Myung, J.; Yoon, S. Selective Enrichment of *Methylococcaceae* versus *Methylocystaceae* Methanotrophs via Control of Methane Feeding Schemes. *Environ. Sci. Technol.* **2024**, *58* (32), 14237–14248.
- (43) Ramoneda, J.; Stallard-Olivera, E.; Hoffert, M.; Winfrey, C. C.; Stadler, M.; Niño-García, J. P.; Fierer, N. Building a genome-based understanding of bacterial pH preferences. *Sci. Adv.* **2023**, *9* (17), No. adf8998.
- (44) Mukherjee, S.; Juottonen, H.; Siivonen, P.; Quesada, C. L.; Tuomi, P.; Pulkkinen, P.; Yrjälä, K. Spatial patterns of microbial diversity and activity in an aged creosote-contaminated site. *ISME J.* **2014**, *8* (10), 2131–2142.
- (45) Grostern, A.; Elizabeth, A. E. Growth of *Dehalobacter* and *Dehalococcoides* spp. during Degradation of Chlorinated Ethanes. *Appl. Environ. Microbiol.* **2006**, *72* (1), 428–436.
- (46) Liang, Y.; Lu, Q.; Liang, Z.; Liu, X.; Fang, W.; Liang, D.; Kuang, J.; Qiu, R.; He, Z.; Wang, S. Substrate-dependent competition and cooperation relationships between *Geobacter* and *Dehalococcoides* for their organohalide respiration. *ISME Commun.* **2021**, *1* (1), No. 23.
- (47) Fernández-Verdejo, D.; Cortés, P.; Guisasola, A.; Blázquez, P.; Marco-Urrea, E. Bioelectrochemically-assisted degradation of chloroform by a co-culture of *Dehalobacter* and *Dehalobacterium*. *Environ. Sci. Ecotech.* **2022**, *12*, No. 100199.
- (48) Yamada, T.; Sekiguchi, Y.; Hanada, S.; Imachi, H.; Ohashi, A.; Harada, H.; Kamagata, Y. *Anaerolinea thermolimos* sp. nov., *Levilinea saccharolytica* gen. nov., sp. nov. and *Leptolinea tardivitalis* gen. nov., sp. nov., novel filamentous anaerobes, and description of the new classes Anaerolineae classis nov. and Caldilineae classis nov. in the bacterial phylum Chloroflexi. *Int. J. Syst. Evol. Microbiol.* **2006**, *56* (6), 1331–1340.
- (49) Cai, C.; Li, L.; Hua, Y.; Liu, H. L.; Dai, X. H. Ferroferric oxide promotes metabolism in *Anaerolineae* other than microbial syntrophy in anaerobic methanogenesis of antibiotic fermentation residue. *Sci. Total Environ.* **2021**, *758*, No. 143601.
- (50) Matturro, B.; Pierro, L.; Frascadore, E.; Papini, M. P.; Rossetti, S. Microbial Community Changes in a Chlorinated Solvents Polluted Aquifer Over the Field Scale Treatment With Poly-3-Hydroxybutyrate as Amendment. *Front. Microbiol.* **2018**, *9*, No. 1664.
- (51) Zhang, C.; Atashgahi, S.; Bosma, T. N. P.; Peng, P.; Smidt, H. Organohalide respiration potential in marine sediments from Aarhus Bay. *FEMS Microbiol. Ecol.* **2022**, *98* (8), No. fiac073.
- (52) Qiao, W.; Jácome, L. A. P.; Tang, X.; Lomheim, L.; Yang, M. I.; Gaspard, S.; Avanzi, I. R.; Wu, J.; Ye, S.; Edwards, E. A. Microbial Communities Associated with Sustained Anaerobic Reductive Dechlorination of  $\alpha$ -,  $\beta$ -,  $\gamma$ -, and  $\delta$ -Hexachlorocyclohexane Isomers to Monochlorobenzene and Benzene. *Environ. Sci. Technol.* **2020**, *54* (1), 255–265.
- (53) Wu, R.; Shen, R.; Liang, Z.; Zheng, S.; Yang, Y.; Lu, Q.; Adrian, L.; Wang, S. Improve Niche Colonization and Microbial Interactions for Organohalide-Respiring-Bacteria-Mediated Remediation of Chloroethene-Contaminated Sites. *Environ. Sci. Technol.* **2023**, *57* (45), 17338–17352.